Colloquia: Channeling 2010

X-ray refraction 3D-simulation software: First approach

L. Allocca([1]), S. B. Dabagov([2])([3]) and L. Marchitto([1])(*)

([1]) *CNR Istituto Motori - Via G. Marconi 8, 80125, Napoli, Italy*
([2]) *INFN Laboratori Nazionali di Frascati - Via E. Fermi 40, I-00044 Frascati, Italy*
([3]) *RAS P.N. Lebedev Physical Institute - Leninsky Pr. 53, 119991 Moscow, Russia*

Summary. — In this work preliminary results on simulation of X-ray propagation in media characterized by low index of both refraction and absorption are reported. A 3D simulation software reproduces parallel X-ray beam colliding the samples while the emerging field distribution is evaluated at the detector place. The simulation code has been structured in order to foresee the different nature of investigating samples and transmitting media. The pictures of the emerging radiation, collected at the detector position, show a good sensibility of the software with respect to the sample parameters pointing it out as a powerful tool to set up arrangements of complex experimental apparatus. The first approach has proved the feasibility of typical Math code application for the analysis of X-ray imaging measurements performed by means of high-flux and low-divergent beams shaped by polycapillary half lens.

PACS 41.50.+h – X-ray beams and X-ray optics.

1. – Introduction

The X-ray radiography technique is a new approach to investigate both the fluid dynamics and the structure of liquid jets, promising to explore deeply inside high dense sprays where laser or visible light-source based techniques are prevented by multi-scattering conditions. However, low X-ray refraction and absorption characteristics of studied materials are limiting us in our investigations. Moreover, it is rather problematic to manage complex sources and detectors typically used at running experiments [1, 2].

In this work a numerical simulation code has been reported, jointly to experimental tests based on the use of conventional laboratory sources combined with polycapillary optical elements. The aim has been to built up an open simulation code where both characteristics and nature of the radiation sources, structure and geometry of the samples,
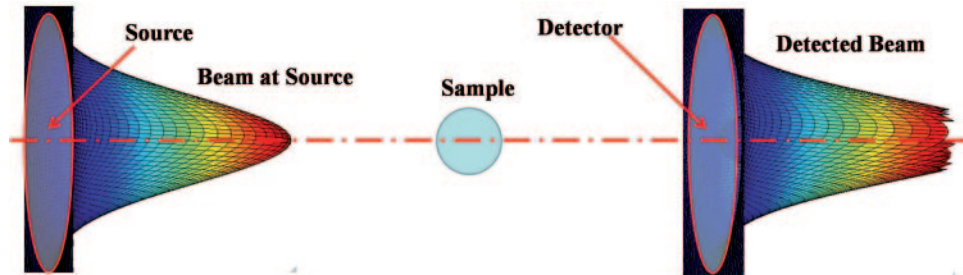
(*) E-mail: l.marchitto@im.cnr.it

Fig. 1. – Sketch of a typical simulation: a spherical sample is aligned with a source and a detector.

and, finally, detectors can be varied enabling in such a way to test a wide possibility of investigating conditions and choose the most effective one.

As a starting condition a 3D simulation software, reproducing soft X-ray absorption by a static sample, has been developed. The source simulates a parallel (or quasi-parallel) X-ray beam. The optical path is in the vacuum and develops from the radiation source to the sample, and subsequently to the detector. A sketch of a typical simulation is shown in fig. 1.

2. – Source

The source geometry is represented by a circular spot. It is possible to select its position and size having determined the radius as well as the coordinates of a centre. The generated beam could be parallel, quasi-parallel, or composed of random rays.

2‘1. *Parallel beam.* – A normalized Gaussian distribution is generated by the formula

$$p(x,y) = e^{-\frac{(x-x_c)^2+(y-y_c)^2}{2\sigma^2}} \tag{1}$$

obtained modifying the classical Gaussian distribution equation

$$p(x) = \frac{1}{\sqrt{2\pi\sigma^2}} e^{-\frac{(x-x_c)^2}{2\sigma^2}}, \tag{2}$$

where x_c and y_c are the source centre coordinates, and σ^2 is the variance. The last one has been optimized to obtain a beam shape as realistic as possible, and it is automatically recalculated by the software at every change of the source diameter in order to preserve the distribution profile. The term in eq. (2), $1/\sqrt{2\pi\sigma^2}$, is missing in eq. (1), adapted for the 3D use, to normalize the $p(x,y)$ function.

This general description of the field distribution is transformed in energy setting but normalized to its maximum energy value.

2‘2. *Random rays distribution.* – Random rays distribution has been generated by linking vector starting points, randomly selected among source grid, to a second one, parallel to the source and coaxial to it. The distance between the circles is fixed. The radius of the second circle is automatically calculated by selecting the maximum angle between the rays and source axis. The rays path is contained in a cone frustum. Vector
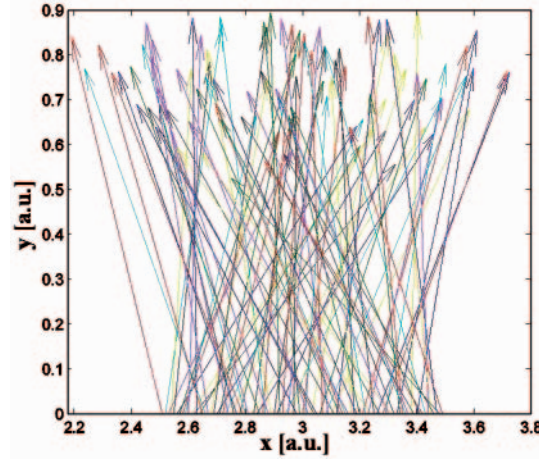
Fig. 2. – Random beam example: 2D source diameter cross-section. 25° maximum divergence angle.

length is constant and it is equal to one (arbitrary unit). A source diameter cross-section is shown in fig. 2.

2˙3. *Mathematical model.* – The refraction index coefficients δ and β (normally characterizing the sample media) depend on the energy of the source that has been taken into account according to the following well-known relation:

$$(3) \qquad n(\omega) = 1 - \delta + i\beta = 1 - \frac{n_a r_e \lambda^2}{2\pi} \left(f_1^0 - i f_2^0 \right),$$

where $f_1^0(\omega)$ and $f_2^0(\omega)$ are the atomic scattering factors of propagating media and the frequency ω; n_a and r_e are the atomic density and the electron radius, respectively. In the code they are collected in a database as the energy function. A 3D Gaussian distribution is adopted to simulate beam divergence if a quasi-parallel one is set (expected value: zero radians, maximum divergence angle is set at the boundary). The electric field $\vec{E}$ of the propagating X-wave changes in the space according to the formula

$$(4) \qquad \vec{E}(\vec{r}, t) = \vec{E}_0 e^{-i(\omega t - \vec{k} \cdot \vec{r})},$$

where

$$(5) \qquad k \equiv |\vec{k}| = \frac{\omega}{c}(1 - \delta + i\beta)$$

is the wave vector.

Substituting eq. (5) in (4), one has

$$(6) \qquad \vec{E}(\vec{r}, t) = \vec{E}_0 e^{-i(\omega t - r/c)} e^{-i(2\pi\delta/\lambda)r} e^{-(2\pi\beta/\lambda)r},$$

where the first exponential factor represents the vacuum propagation part, while the second is the phase shift; and the third corresponds to the wave intensity decay due to

the absorption [3, 4]. Finally, the average intensity is estimated as

$$(7) \qquad\qquad \bar{I} = \bar{I}_0 e^{-(4\pi\beta/\lambda)r}.$$

It is possible to estimate both modulus and phase in each point compatibly with the accuracy rate used. However, these values are estimated at the initial, final and medium sample-interface positions in order to speed up the software.

3. – Samples and sample-media interface

The simulation code has been structured in order to foresee the different nature of the investigating samples and the transmitting media. In fact, it is possible to specify the chemical formula of the medium as well as that of the samples to evaluate the refraction index and its coefficients. In this case the medium is set as a vacuum by default ($n = 1$). Different geometries can be chosen for the sample: parallelepiped, prism, sphere or a collection of spheres with the possibility to define the center and the diameter of each one.

A specific subroutine generating random groups of samples of a defined shape is under development to simulate drops of different shapes or clouds of droplets (for instance, conical-like shapes for injected fuel sprays).

The propagating X-ray from the source impacts the sample with a wave vector $\vec{k}$ forming the angle with the normal to the sample surface depending on the incident point. The code evaluates the refracted vector and point out direction inside the sample according to the Snells law. A 3D equation system is applied and the emerging wave vector $\vec{k}$ of the refracted wave direction gives the new impact point at the sample/medium surface. A new incident angle with respect to the normal to the surface is established and a new 3D equation system gives the direction of the emerging wave from the droplet. The direction of the last k vector enables to calculate the intersection with the detector plane giving the diffraction figure of the incident X-ray on the interposed sample.

4. – Detector

Field distribution at the detector plane is evaluated. The detector is simulated by a circular spot but no spatial limits have been posed. Diameter and centre position are defined by the user. All the field components estimated at the detector plane, which are out of the spot, are rejected.

5. – Results

Absorption and phase-shift have been evaluated by running the software. Here are reported results concerning a parallel beam (cross-section diameter of 10 mm), which impacts against three different samples: a sphere, a plane sample, and triangular section prismatic sample. The outgoing beam is collected by the detector, which is characterized by the same source dimensions. The beam has a photon energy peak sizing 6000 eV. The source, sample and detector are aligned. The selected medium is the vacuum ($n = 1$).

The initial electric field distribution is normalized and the waves are supposed to have the same polarization at start.

Figure 3 shows the normalized intensity distribution, $\bar{I}/\bar{I}_0$ recorded at the detector. The calculated average intensities at detector are coherent with the expected ones for
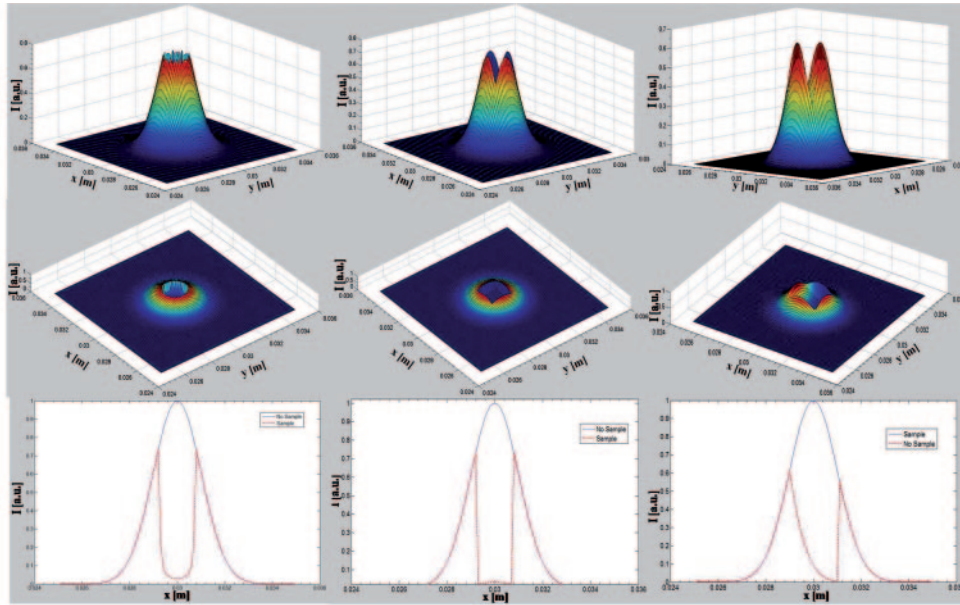
Fig. 3. – Detected Signal: 3D (lines 1 and 2) and 2D detector diameter cross-section graphs (line 3) concerning the impact with spherical sample (left), plane sample (centre), prismatic sample (right).

all the explored cases. Particularly, looking at detector diameter cross-section profile shown in fig. 3 (right), it is possible to appreciate the increasing trend of intensity where a linearly increasing thickness is crossed by the beam; the trends are not the same due to the Gaussian distribution of the beam at the source. The right prismatic sample has been selected to simulate a variable absorption sample, since the evaluated refraction angle is negligible.

The spherical sample has a diameter of $1.5\,$mm, the selected material is carbon. The code estimates the following refraction coefficients: $\beta = 3.89588521 \cdot 10^{-8}$ and $\delta = 1.2743013 \cdot 10^{-5}$. The maximum intensity absorption, estimated on the source/detector axis, is about 97%.

The plane sample is cerium made, it has a thickness of $10\,\mu$m, and it has a square section area with the side of $1.5\,$mm, with the following refraction coefficients: $\beta = 5.696590644 \cdot 10^{-6}$ and $\delta = 2.643993703 \cdot 10^{-5}$.

The prismatic sample is carbon made, it has an isosceles right triangle basis, it is positioned to have one of the two equal side faces aligned with the source axis. Hence, the thickness crossed by the beam is linearly increasing if it is looked at from the source cross-section plane.

Tests on spherical sample by generating rays random instead of the quasi-parallel beam have been conduced, the working conditions are reported in table I. First code runs highlight a like-real system behavior. The detected diameter decreases by increasing the sample distance from the source at negative divergence, as shown in fig. 4.

TABLE I. – *Random rays distribution: working conditions.*

	Sample centre position (m)	Measured diameter (m)
Source diameter 0.10 m		
Detector diameter 0.08 m	0.025	0.0224
X-ray path 0.10 m	0.050	0.0262
Sample diameter 0.03 m	0.075	0.0282

6. – Conclusion

In this work, a simulation software reproducing X-ray absorption by static sample has been developed. Different source configurations, sample chemical compositions and shapes have been tested. First results highlight a coherent estimation of the wave decay.

Parallel and quasi-parallel beams have been reproduced to simulate those emitted by source and collimated by means of polycapillary optics. Different sample shapes and substances have been combined to test the code. Results concerning a carbon spherical sample, a cerium plane sample have been reported, demonstrating a good model accuracy and a like-real behavior. A carbon prismatic sample has been used to simulate a linearly variable absorption one, by exploiting the very low refraction angle. The normalized intensity distributions $\bar{I}/\bar{I}_0$ are coherent with the expected one. The results have pointed out a good sensitivity of the system extended to low absorption samples.

Random rays distribution code has been successfully tested. The maximum angle between the rays and the source axis can be set, allowing to generate rays just inside a cone frustum. The signal at detector is correctly influenced by the set angle and by the relative position of the sample respect to the source and to the detector.
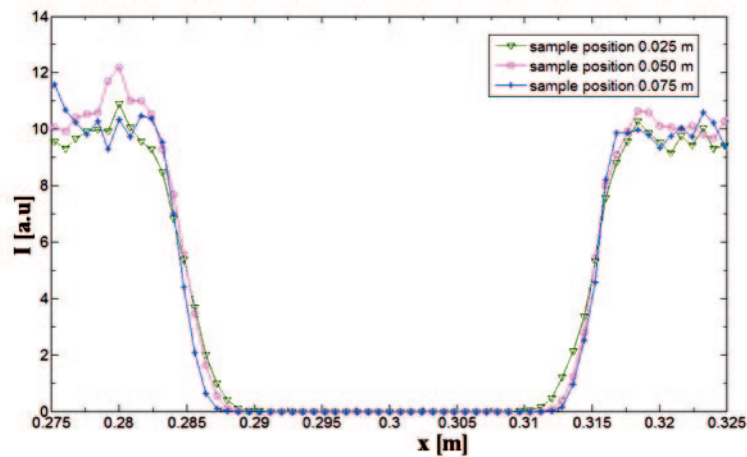

Fig. 4. – Random rays beam: diameter cross-section signal detected at the detector.

In future works, it will be basic to simulate the X-rays behavior inside of the lens allowing an accurate source simulation [4]. Final aim of the code will be to forecast the X-ray absorption by high dense fuel sprays. On the one hand, the code is enough sensitive to fuel droplets, that are hydrocarbon chains characterized by very low absorption. On the other hand, the spray is composed of thousands of droplets of size 5–15 μm.

REFERENCES

[1] WANG J., *X-ray Vision of Fuel Sprays*, *Journal of Synchrotron Radiation*, edited by International Union of Crystallography (2005), pp. 197-207.
[2] ALLOCCA L., MARCHITTO L., ALFUSO S., HAMPAI D., CAPPUCCIO G. and DABAGOV S. B., *Gasoline Spray Imaging by Polycapillary X-Ray Technique*, in *X-Ray Optics and Microanalysis: Proceedings of the 20th International Congress. AIP Conf. Proc.*, Vol. **1221** (2010), pp. 191-195.
[3] DABAGOV S. B and MARCELLI A., *Appl. Opt.*, **38** (1999) 7494.
[4] ATTWOOD D., *Soft X-rays and Extreme Ultraviolet Radiation: Principles and Applications* (Cambridge University Press, New York) 1999, pp. 55-69.